Observation of Multiple GeV Solar Energetic Particles from the 6 Nov. 1997 Event Using Milagrito

A.Falcone, R.Atkins, W.Benbow, D.Berley, J.Bussons-Gordo, M.L.Chen, D.G.Coyne, R.S.Delay, B.L.Dingus, D.E.Dorfan, R.W.Ellsworth, L.Fleysher, R.Fleysher, G.Gisler, J.A.Goodman, T.J.Haines, C.M.Hoffman, S.Hugenberger, L.A.Kelley, I.Leonor, M.McConnell, J.F.McCullough, J.E.McEnery, R.S.Miller, A.I.Mincer, M.F.Morales, P.Nemethy, J.M.Ryan, F.Samuelson, M.Schneider, B.Shen, A.Shoup, C.Sinnis, A.J.Smith, G.W.Sullivan, T.N.Thompson, T.Tumer, K.Wang, M.O.Wascko, S.Westerhoff, D.A.Williams, T.Yang, G.B.Yodh
(The Milagro Collaboration)

ABSTRACT

Milagrito was an extensive air shower observatory which operated as a prototype for the larger Milagro instrument. It operated from February 1997 to May 1998. Although Milagrito was originally designed as a high energy (>100 GeV) water Cherenkov gamma ray observatory, it could also be used to study solar energetic particles (SEPs) from the Sun. In a scaler mode, it was sensitive to muons and small showers from hadronic primary particles above ~4 GV. Milagrito also operated in a shower mode which had increased sensitivity due to its ability to reconstruct event directions, but this mode required primary particles of higher energy. In its scaler mode, Milagrito registered a ground level enhancement associated with the 6 November 1997 SEP event and X9 solar flare. At its peak, the enhancement was 22× background RMS fluctuations. Based on comparisons to neutron monitor and satellite data, we conclude that the differential flux of energetic protons from this event followed a rigidity-power-law spectrum which became steeper above 4 GV, and that the acceleration site was in the low corona (~2 solar radii).

1. Introduction

Particle acceleration beyond 1 GeV due to solar processes is well established (e.g. Meyer et al. 1956, Parker 1957). However, few data exist demonstrating acceleration of particles beyond 5 GeV (Chiba et al. 1992, Lovell et al. 1998). The energy upper limit of solar particle acceleration is unknown but is an important parameter because it relates not only to the nature of the acceleration process, itself not ascertained, but also to the environment at or near the Sun where the acceleration takes place. Due to their small size, space-based instruments are inefficient at measuring the low fluxes of particles above ~1 GeV. However, neutron monitors become efficient at these energies. Neutron

monitors provide an integral measurement of the particle intensity above a threshold determined by the location of the monitor. To study the solar energetic particle (SEP) intensity above the equatorial neutron monitor threshold, other instruments are necessary.

Coronal mass ejections (CMEs) and solar flares are frequently accompanied by SEPs, but the details of the acceleration process(es) continue to elude researchers. Although SEP events are frequently categorized as either gradual or impulsive (Reames 1999, Gosling 1993), some events do not seem to fit neatly into either category (Mobius et al. 1999). Gradual events generally exhibit greater fluxes of SEPs over long time scales and tend to be associated with long-duration type II/IV radio emission, coronal ion abundances, and low electron-to-ion ratios. On the other hand, impulsive events typically exhibit smaller fluxes of SEPs over shorter time scales. They also tend to be associated with large electron-to-ion ratios and enhancements in heavy ions and ^{3}He. Fast (v>400 km/s) CME driven coronal and interplanetary shocks are generally thought to be the acceleration mechanism for the gradual events (Lee 1997, Kahler 1992), while the impulsive events are frequently thought to originate at the flare site (Reames 1999).

Milagro and Milagrito are capable of fulfilling the function of studying these high energy SEP events by operating at higher energies with large areas. Milagrito observed (and Milagro presently observes) a large fraction of the secondary particles from air showers by utilizing the water Cherenkov technique in a large, water-filled pond. This increased shower particle absorption relative to that of traditional extensive air shower arrays, which are insensitive below several hundred GeV, contributes to the lower energy threshold of Milagro and Milagrito. This technique also leads to an effective area that is more than three orders of magnitude greater than that of neutron monitors above ~3 GeV. With an intrinsic energy threshold for protons of ~4 GV, due to the shielding effect of the Earth's geomagnetic field, Milagro/ito data can also complement that of the neutron monitor network. An increased sensitivity to high-energy, anisotropic events can also be achieved when Milagro/ito is able to reconstruct the primary particles' incident direction.

On 6 November 1997 at 11:49 UT, an X9 flare with an associated coronal mass ejection (CME) occurred on the western hemisphere of the Sun. This event was well observed with many instruments, and it exhibited both gradual and impulsive characteristics. The GOES-9 satellite detected energetic protons in excess of 100 MeV, as well as hard X-rays. Yohkoh recorded impulsive gamma-ray emission up to 100 MeV for approximately 5 minutes, along with the presence of gamma ray lines (Yoshimori et al. 2000). LASCO detected the launch of the CME from the Sun, and the speed of the leading edge was estimated to be in excess of 2000 km/s. Type II and IV radio emission were also observed during this event. Using ACE measurements, Cohen et al. (1999) and Mason et al. (1999) reported exceptionally hard ion spectra above 10 MeV/nuc. Furthermore, Fe and ^{3}He enhancements (Fe/O~1 and ^{3}He/^{4}He~4× coronal) were evident in the interplanetary particle populations. These values are greater than those expected for a gradual event, but the enhancements are not as great as those found in many impulsive events.

There were also ground-based measurements of this event. Many of the instruments in the world-wide network of neutron monitors registered a ground level enhancement (GLE) in response to high energy (>1 GeV) protons (Duldig et al. 1999). The rate increase began shortly after 12:00 UT with an anisotropic component, but the distribution became almost isotropic by the time of maximum, approximately 45 minutes after the onset (Lovell et al. 1999). The Climax neutron monitor, located < 400 km north of the Milagrito site with a vertical cutoff rigidity of ~3 GV, also recorded an increase.

2. Milagrito Instrument Description

Milagrito was located near Los Alamos, NM at an elevation of 2650 m (750 g/cm^2 atmospheric overburden). It operated as a prototype for the Milagro instrument from February 1997 to May 1998 (Atkins et al. 2000; McCullough et al. 1999). The detector was composed of 228 upward-facing photomultiplier tubes (PMTs) submersed in 1-2 meters of "clean" water (attenuation length of about 5 m). These tubes were placed within an 80×60×8 m pond, under a light-tight cover, in a square grid pattern with 3 m spacing between each PMT. When an energetic hadronic particle or gamma ray is incident on the Earth's atmosphere, it can trigger an extensive air shower (EAS) that propagates downward in the form of a thin (~1-3 m) "pancake-like" plane of secondary particles. Upon entering the water of the Milagrito pond, the charged particles from the EAS produce Cherenkov light in characteristic 42˚ light cones. These Cherenkov photons are then detected by the PMT array. The gamma rays in the EAS undergo both Compton scattering and pair production when they enter the water, thus contributing to the Cherenkov photons detected in the pond. With this water Cherenkov technique, a large fraction of the shower particles can be detected, and a low threshold energy is achievable.

Designed as a Very High Energy (VHE) gamma ray observatory, Milagrito's baseline telescope mode was sensitive to extensive air showers from primary hadrons and gamma rays above ~100 GeV. In its baseline telescope mode, Milagrito required 100 PMTs to trigger in order for the data acquisition hardware to record an event. In this "100 PMT" mode of operation, a PMT triggers when its pulse height exceeds a "low" threshold, corresponding to ~0.25 photoelectrons. For each event, the time and pulse height in each PMT were recorded. The time-over-threshold technique was used to measure pulse height with a dead time of less than 4%. Once these data were recorded, they could be used to reconstruct the incident direction of the primary particle with a resolution of less than 1˚. The hadron-induced showers were treated as background for the baseline gamma ray telescope mode, but these events were treated as a signal for the purposes of solar and cosmic ray physics.

In addition to recording these "100 PMT" mode events, thus operating as a telescope, Milagrito also had a scaler mode of operation. This mode of operation is similar to that of a neutron monitor. It records a time-integrated measurement that corresponds to the rate of single PMT hits in the pond. In this scaler mode of operation, a

PMT was considered to be “hit” when its pulse height exceeded the “high” threshold, corresponding to ~7.6 photoelectrons. This “high” threshold output has considerably less background fluctuation than the “low” threshold output used for the “100 PMT” baseline mode. This is important when considering the large number of smaller and unreconstructable events registered in the scaler mode. The PMTs were separated into 15 “patches,” and the scaler mode counted the number of patches that registered at least one hit during a ~45 ns interval. Thus, an event that triggers only one PMT constitutes a count in the scaler mode, and an event that triggers several PMTs (within ~45 ns of each other) within one patch of 16 PMTs will also constitute only one count in the scaler mode. The number of scaler hits was read with a period of 1 second.

Since the energy range most likely to be of primary interest to solar physics is <100 GeV, the scaler mode of Milagrito is extremely useful, despite the fact that imaging is not possible with the scaler mode. A substantial fraction of the scaler rate recorded by Milagrito was due to muons, and an integral measurement above a hardware-defined threshold is performed. These data provide an excellent high energy complement to the network of neutron monitors.

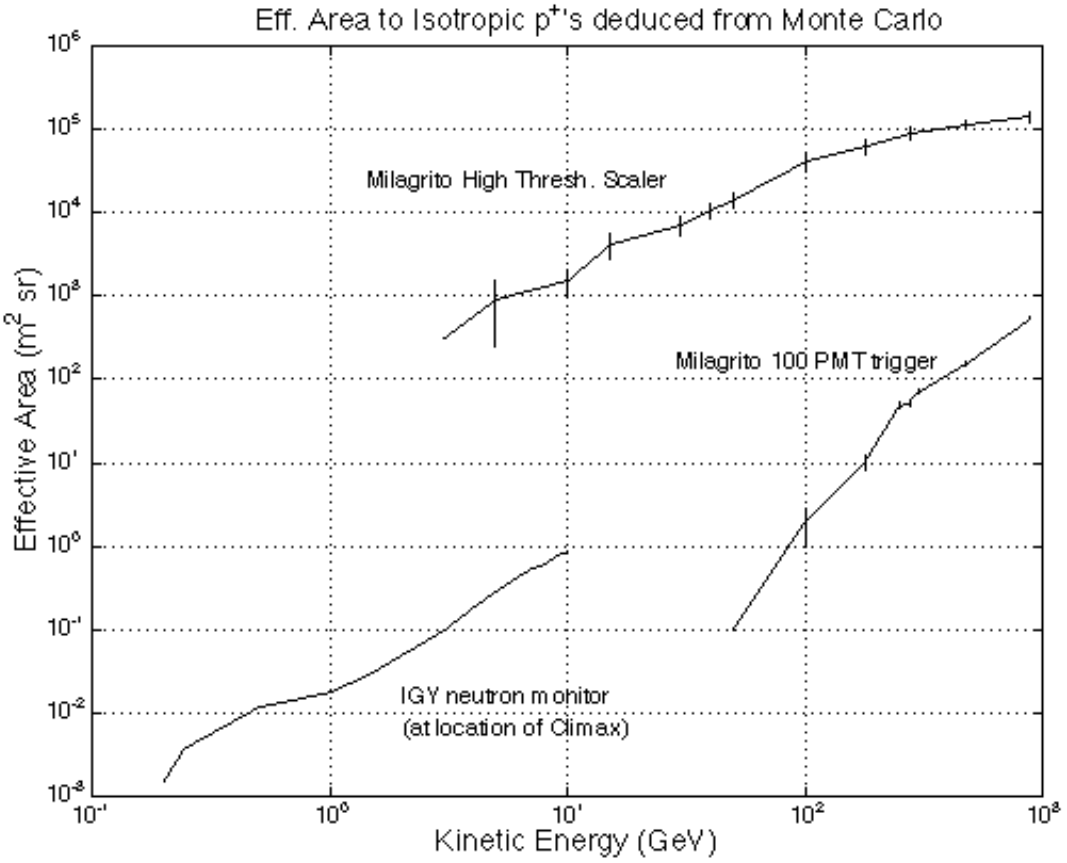

Fig. 1 – Effective area of Milagrito to isotropic protons incident on the top of the Earth’s atmosphere, with an IGY neutron monitor for comparison. These calculations are based on Monte Carlo proton events thrown over zenith angles of 0˚-60˚, with extrapolated values used for zenith angles from 60˚-90˚.

With Monte Carlo calculations, we computed the effective areas of Milagrito to protons incident on the atmosphere isotropically, at zenith angles ranging from 0^o-60^o (Figure 1). The effective area from 60^o-90^o was estimated by extrapolating the area curve from the 0^o-60^o range. In the absence of effects specific to large zenith angles, the majority of the contribution to the scaler mode efficiency comes from zenith angles below 60˚. For protons at 50 GeV, this can be seen in figure 2. Since cosmic ray showers were not simulated between 60^o-90^o due to limitations of the software and time, effects that are present only at large zenith angles are not reflected in these effective area curves (see section 3.2). While this could have a significant impact on the analysis of the shower mode data, it should not significantly affect the scaler mode data analysis. The complete simulation of the detector response was performed in two steps. The initial interaction of the primary particle with the atmosphere and the generation of secondary particles was simulated with the CORSIKA air shower simulation code (Heck et al. 1998). The primary particles and shower particles are tracked through the atmosphere, which is stratified into five horizontal layers. When the particles initiate a reaction or decay, the secondary particles are also tracked through the atmosphere. Electromagnetic interactions are simulated using EGS 4 code. For the hadronic interactions, the VENUS code is used at high energies, and GHEISHA is used at low energies (<80 GeV). The second step was to simulate the response of the detector itself using GEANT (CERN 1994).

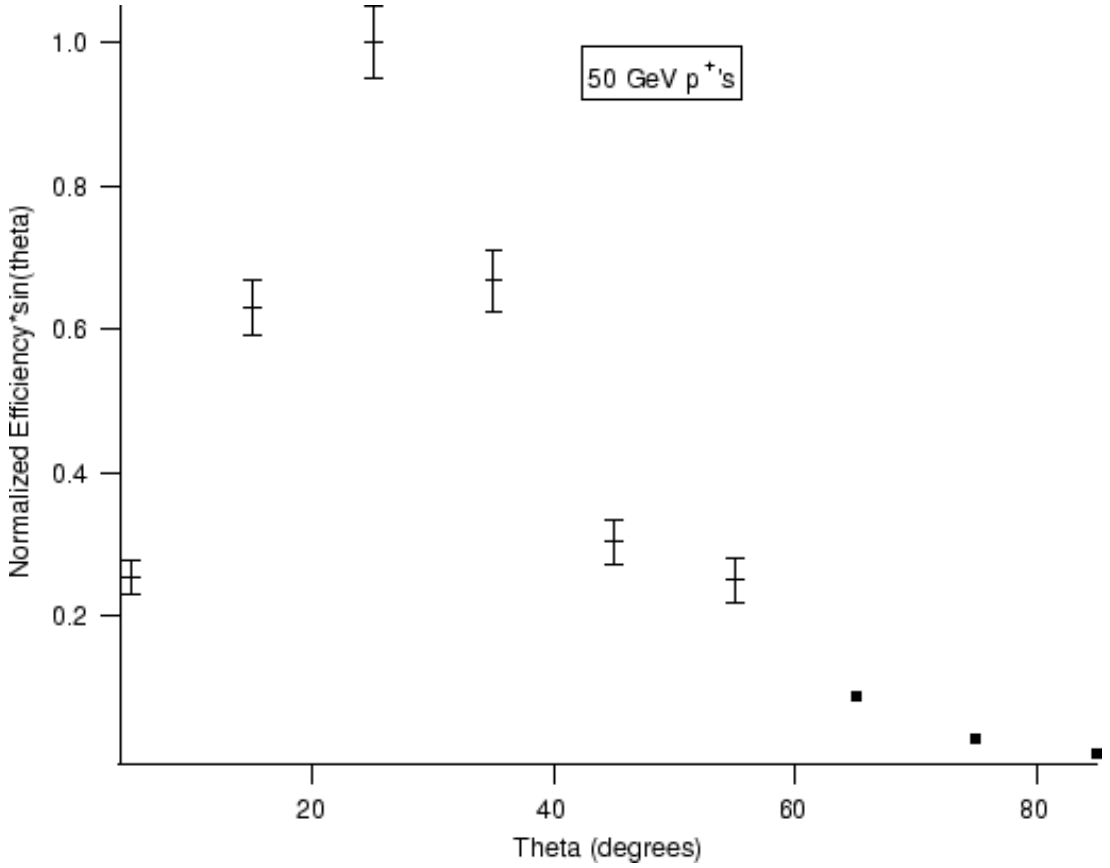

Fig. 2 – Milagrito scaler mode differential efficiency to 50 GeV protons (from Monte Carlo) normalized to 25˚ and plotted as a function of zenith angle. Points above 60˚ are extrapolated using a functional fit to lower θ points. The contribution from θ>60˚ is shown

The systematic errors of the instrument response have been estimated by folding the known cosmic ray spectrum through the calculated response. This results in a theoretical value for the instrument's rate due to galactic cosmic rays, which comprise most of the instrument's background rate. The measured background rate in Milagrito matches this predicted value to within a factor of ~3. While this provides us with a reasonable level of confidence in the calculated effective area curves, there are still some lingering concerns. There are some concerns with using GHEISHA to simulate showers from primary particles with energies below ~20 GeV (Heck 1999). For these lower energy primary particles, it is possible that the sum of the secondary shower particles' energies can be as much as 20-30% greater than the energy of the primary hadron. While a reasonable agreement (factor of ~3) between the predicted and the measured cosmic ray rates in Milagrito shows that the effective area systematic errors are reasonably small, we are unable to assess the effect of using GHEISHA at energies below ~20 GeV.

At 10 GeV, Milagrito's scaler mode effective area is ~3 orders of magnitude greater than that of a sea level neutron monitor, with the effective area rising rapidly with energy. The areas in Fig. 1 were calculated using Monte Carlo events whose shower cores were thrown randomly over a large area surrounding the Milagrito pond. To ensure that the Monte Carlo showers were thrown over a large enough area, we progressively increased the throw area until the effective area reached an asymptotic value. This occurred at approximately 7000×7000 m^2. Figure 3 illustrates the relationship between Milagrito's predicted effective area and the shower-core throw area for 50 GeV protons. We note that the effective area of Milagrito has a significant contribution from hadronic

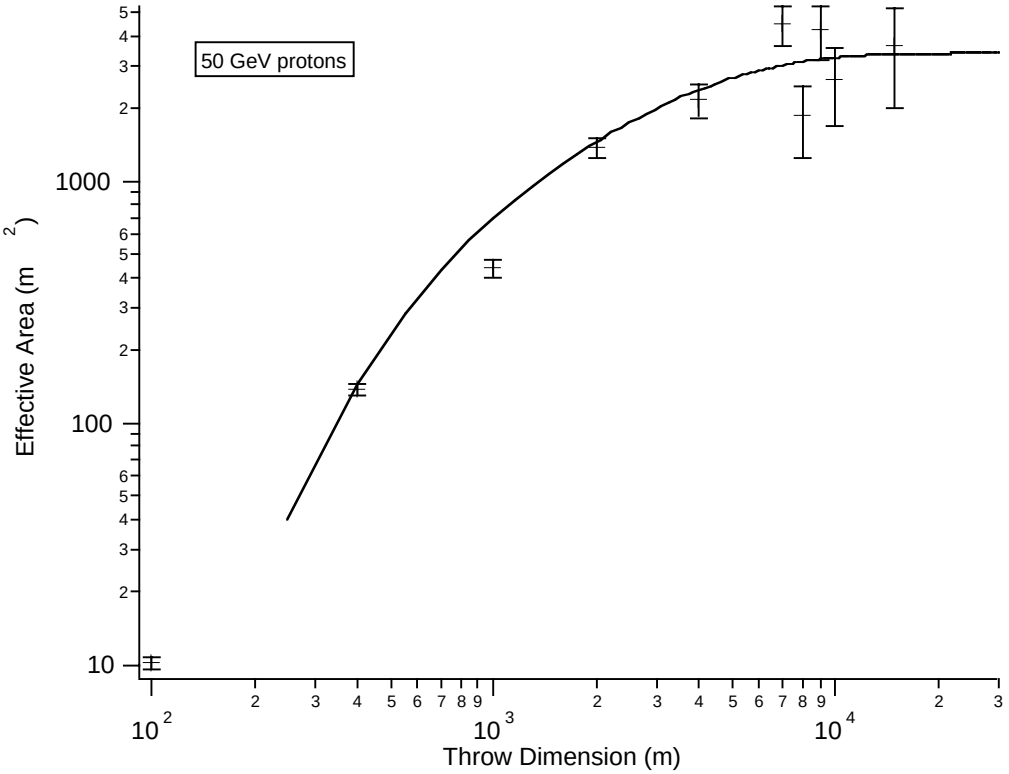

Fig. 3 – An example of the relationship between effective area and the spatial dimensions over which the Monte Carlo throws the shower cores. An asymptotic value is approached

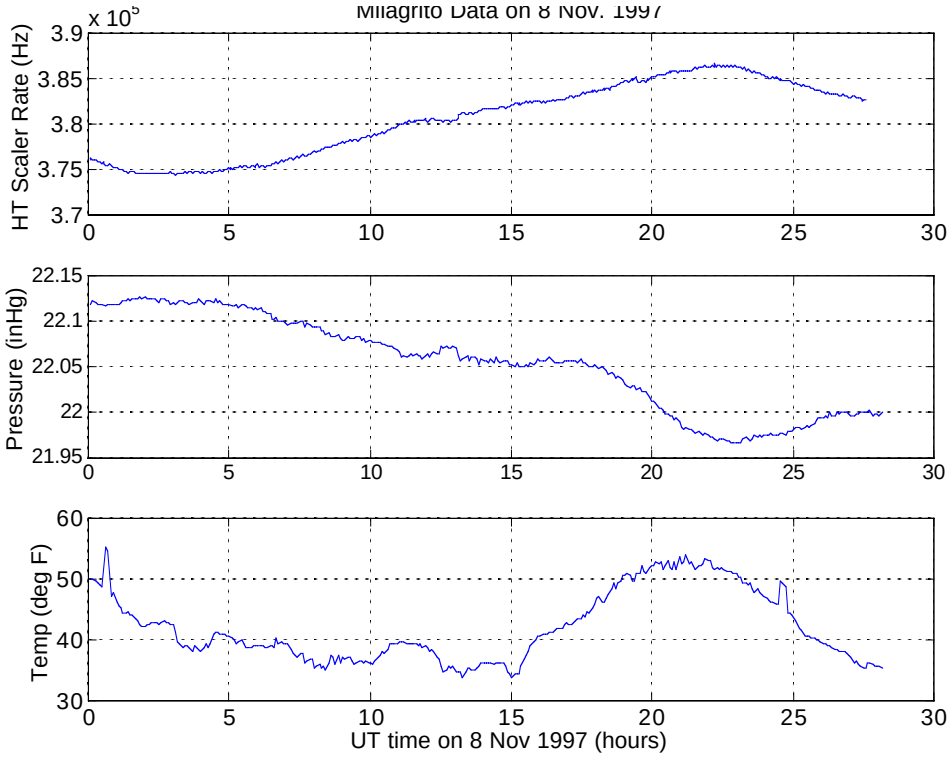

Fig. 4 – Typical diurnal fluctuations in Milagrito scaler rate during a time period which is relatively free of instrumental anomalies.

showers with cores far (> 3 km) from the detector. This effect increased the estimated effective area at ~5-100 GeV by ~3 orders of magnitude relative to earlier estimates (Falcone et al. 1999, Ryan et al. 1999). Our confidence in these revised effective area curves is bolstered by the fact that they predict the instrument's background rate due to cosmic rays to within a factor of ~3.

To properly apply these calculations to the analysis of Milagrito data, one must first correct the ground level scaler rates for pressure, temperature, and other diurnal effects (Hayakawa 1969). Typical background cosmic ray rate fluctuations on a time scale of ~1 day are shown in figure 4. Although this is the pressure at ground level, which is not as critical as the measurement of pressure at higher altitudes in the atmosphere, one can easily observe the increase in background rate as the pressure decreases as a result of the decrease in the atmospheric overburden. Atmospheric temperature also effects the background rate, but this smaller effect can not be seen in the figure due to the overwhelming pressure variation. We have begun to estimate these correction factors for Milagro/Milagrito, and we find them to be reasonably consistent with past work with muon telescopes (Fowler et al. 1961). However, these corrections are less important for transient events that rise above background quickly and have short durations.

3. Observations of 6 November 1997 Event Using Milagrito

The scaler mode and the "100 PMT" mode of Milagrito can be treated as independent data sets.

3.1. *Scaler Mode Observations*

In its scaler mode, Milagrito measured a rate increase coincident, within error, with the increase observed by Climax (see figure 5). If one accounts for the background meteorological fluctuations that are present, the event duration and time of maximum intensity, as seen with Milagrito, are also consistent with that of Climax. The magnitude of the scaler rate increase is ~22 times the RMS fluctuations of the instrument's background using 160 second time bins. The background scaler rate prior to the event

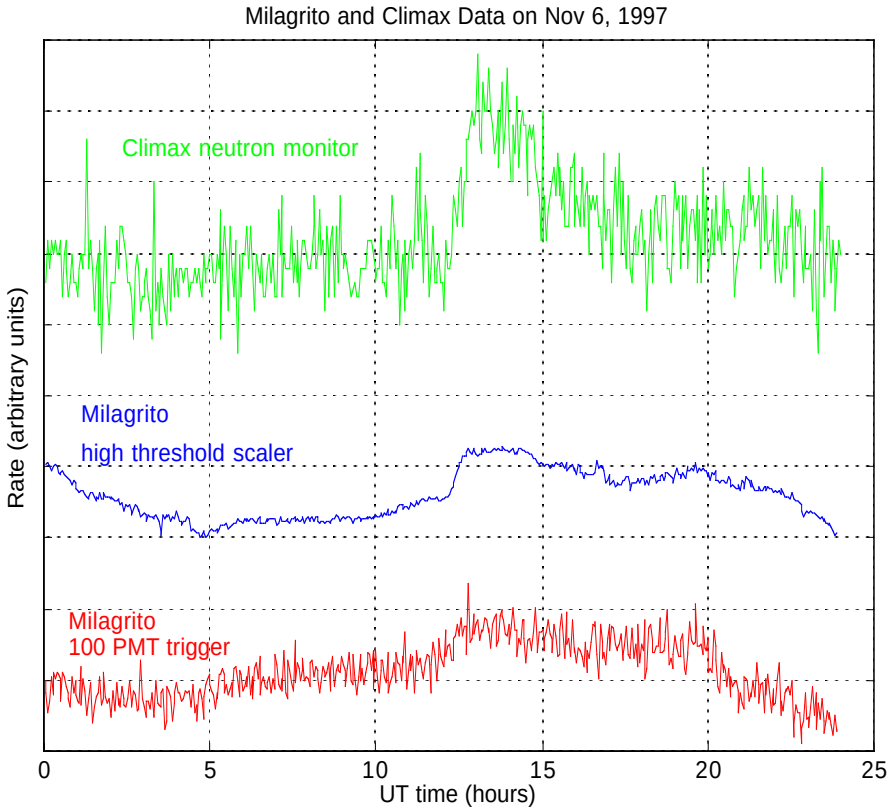

Fig. 5 – Milagrito rate history plotted over the same timescale as the nearby Climax neutron monitor. The high threshold scaler rate increase of Milagrito was coincident with the rate increase observed by Climax. Diurnal background variations are also visible in the Milagrito data.

was ~375 kHz, and the event produced a rate increase of ~0.5 % from the onset to the time-of-maximum. The RMS of observed background fluctuations, which is

approximately ± 84 Hz, is nearly twice that expected from Poisson statistics. These larger fluctuations may be a result of effects such as meteorological fluctuations in the upper atmosphere and at the Milagro site. We also estimated the chance probability of an event rate increase of this magnitude, over this time scale, by looking at the data over the lifetime of Milagrito. There were only two other rate increases of at least this magnitude during the 15 month (~20% dead time due to maintenance, etc.) lifetime of the instrument. One of these is a possible light leak, and the other has been identified as a power up transient effect. It has been found that the upper limit of the probability for a chance rate increase with a magnitude and timescale similar to that of the 6 Nov.1997 event is $\sim 2\times10^{-4}$.

We note that the scaler rate plotted in figure 5 does not include one of the 15 patches of the detector. This historically noisy group of PMTs, located within patch 7, exhibited an unrelated instrumental rate increase a few hours after the onset of the CME related rate increase. This type of instrumental rate increase (referred to as "flashing" and thought to be caused by arcing in the base or light emission in the tube) is common in some clusters of PMTs, but it can be identified and corrected for based on its localized spatial characteristic. A "flasher" will cause a disproportionate rate increase in a local cluster of PMTs, but an air shower signal will cause a more uniform increase over the entire pond. During the rate increase on 6 November 1997, all of the patches except for patch 7 experienced a uniform rate increase with an average increase of 0.48% and a standard deviation of 0.08%. Patch 7 experienced a rate increase of 1.1%. After studying the uniformity of the signal over the pond in this way and analyzing the instrument's behavior over its lifetime, we concluded that most of this instrumental increase could be attributed to patch 7 and that the remaining rate increase was of solar origin.

3.2. *100 PMT Mode Observations*

The 100 PMT shower trigger rate also experienced an increase, although the significance was not as great as that in scaler mode. The magnitude of the rate increase signal to background fluctuations in shower trigger mode was ~10% of that in the scaler mode. We expected that the shower trigger would have a smaller response to an event such as this, since the shower trigger has a higher threshold energy and has less effective area. It is not yet clear which of several possible mechanisms initiated the signal in the 100 PMT shower trigger, so the detector's sensitivity to several possible mechanisms is being investigated. Some of the explanations for the shower mode "signal" that have been considered are isotropic proton primaries (such as those that caused the high threshold scaler increase, but with much higher energies), instrumental effects known as "flashing" PMTs, and high zenith angle muons. The magnitude of these effects influences the systematic errors in the analysis.

This signal does not appear to conform to known instrumental effects, such as "flashing" PMTs. Flashers, which are caused by light emission at the base and/or in the

tube of the PMT, are a common problem with water Cherenkov detectors. There are three known forms of flashers in the Milagrito data that could, in theory, contribute to the 100 PMT signal. One of these forms of flashers is not present at anytime during the event. Another form of flasher, the same one that causes the high rate flashing in patch 7, is not present in the 100 PMT mode during the onset of the event, although particularly high rate flashing did occur several hours later within patch 7. The third form of flasher is present during the onset of the event, but this flashing is present before and after the event as well. Since the flashing remains constant prior to and throughout the event, it cannot be responsible for the observed rate increase.

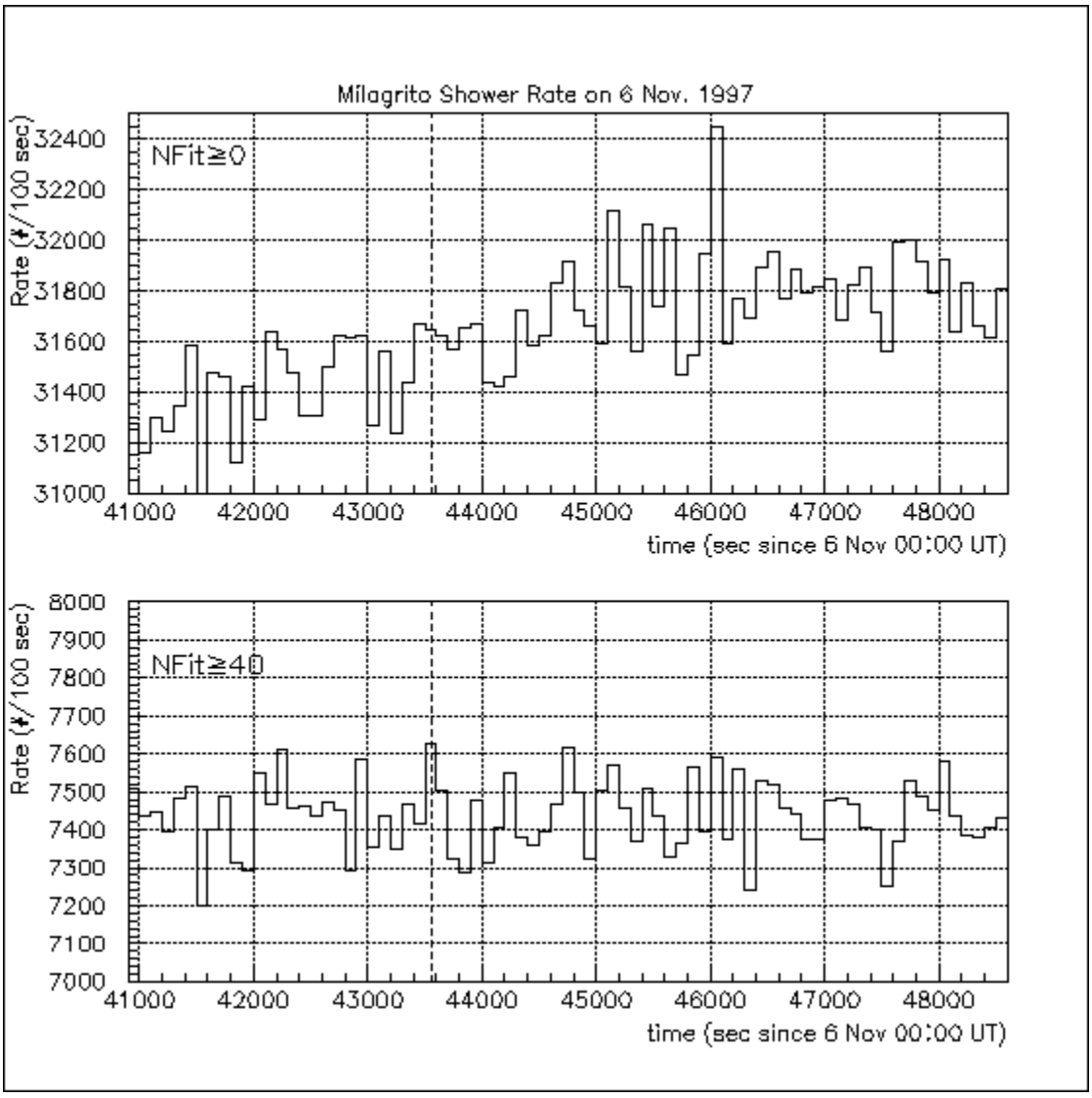

Fig. 6 – Milagrito 100 PMT shower mode rate history at the time of the GLE. The top panel includes all events. The bottom panel, which displays no rate increase, includes only the events for which >39 tubes were suitable for use by the angle fitter. The dashed line is the event onset time according to the high threshold scalers.

Although this slight increase could have been caused by isotropic, very high energy primaries (>100 GeV) to which the effective area curve in figure 1 corresponds, it

is unlikely. Evidence for this can be found by looking at the quality of the air shower fit to a particular incident angle during the "event." Although 100 PMTs trigger the "100 PMT" air shower mode, not all of these PMTs are suitable to be used in the angular reconstruction, also known as "fitting" the event. For example, some PMTs may trigger significantly later or earlier than expected relative to others, thus giving the impression that there is no coherent shower plane. Individual PMTs that contributed disproportionately to the χ^2 of the fit or had a low pulse height were not included in the fitting procedure. For example, if a PMT contributes > 9 to the χ^2 of the fit during the first iteration of the fitting procedure, then it is not used. For more detail on the fitting procedure, see Atkins et al. (2000). The events that caused the shower mode increase on 6 Nov. 1997 all had a low number of PMTs that were suitable for the fitting procedure (see figure 6), and many events could not be fit at all. If this rate increase was due to an

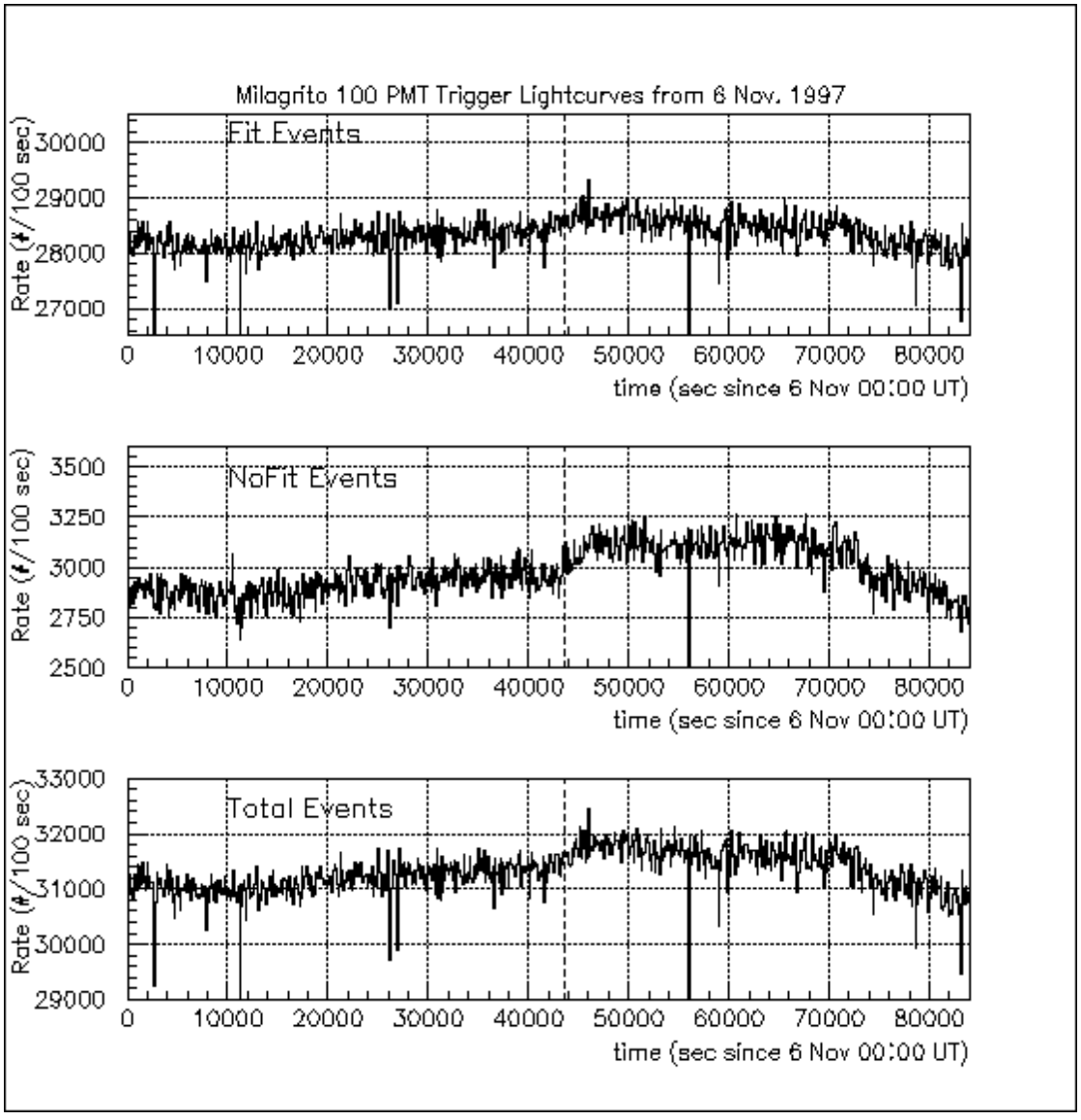

Fig. 7 – Comparison of the 100 PMT mode time histories for fittable and unfittable events. It is apparent that the ratio of events that cannot be fit to events that can be fit increases during the time of the event. (The dashed line marks the onset according to the high threshold scalers.)

isotropic proton distribution, as that modeled between zenith angles of 0^o-60^o, then greater numbers of "fittable" PMTs would be expected since these events lead to "pancake-like" shower fronts, which have a characteristic time delay from one PMT to another. We also see (figure 7) that the fraction of events that cannot be fit increases as the event progresses. Furthermore, if this increase was due to isotropic protons, then a very hard spectrum ($P^{-2.5}$, with ~90% of the events from >200 GeV) is necessary to explain the increase. This spectrum would conflict with the spectrum inferred from the Milagrito high-threshold scaler rate increase, as well as neutron monitor and satellite data.

There is another potential mechanism by which primary protons can trigger the shower mode. High zenith-angle protons leading to secondary muons arriving from nearly horizontal directions could trigger the detector. These events were not simulated beyond 60^o. The increase in the rate of "unfittable" events as the event progresses (figure 7) is evidence for high zenith-angle muons being the cause of the air shower "signal." We determined that the majority of "unfittable" events in the background rate could be attributed to muons from zenith angles > 83˚, thus it is known that this mechanism can cause a trigger in the 100 PMT mode. The efficiency of this mechanism for converting a high-zenith-angle proton into a high-zenith-angle muon, and subsequently triggering the 100 PMT mode, is not known. If horizontal muons contributed to this signal, they would have been the result of high energy proton primaries (>30 GeV), based on estimates of muon losses in the atmosphere, but the effective area curve in figure 1 would not apply to this triggering mechanism. In order to determine the spectrum of the primary protons associated with this mechanism, extensive and time consuming simulations will have to be completed.

Until more studies and simulations beyond 60˚ are performed, the details of the 100 PMT shower mode "signal" cannot be understood. Presently, the work on this 100 PMT "signal" remains inconclusive. We, therefore, restrict our analysis to the scaler rate increase, based on the belief that if the 100 PMT rate increase is of solar origin, it arises from a response characteristic of the instrument that we have not studied thoroughly. Work on understanding the instrument response to primary particles beyond 60˚ is underway.

Proton Spectrum

The high-threshold scaler rate increase of Milagrito can be used to derive characteristics of the primary proton spectrum. We do this by folding a trial power law spectrum of protons through the response of the instrument. The trial power law spectrum is of the form:

$$f = C(P/P_o)^{-\alpha} ,$$

where P is rigidity [GV] and f is the differential proton flux [m^{-2} s^{-1} sr^{-1} GV^{-1}]. The expected rate increase in the detector is then found by numerically integrating:

$$R = \int_{P_{cutoff}}^{\infty} f(P) A_{eff}(P) dP$$

The parameters of the trial spectra, C and α, are then varied until a good fit to the measured rate increase is achieved. By only using the high-threshold scaler rate in this analysis, a range of acceptable values for C and α is determined. In order to uniquely determine the parameters, another detector with a different response is required.

Two assumptions that are present in this analysis should be mentioned. We make the standard assumption that the geomagnetic rigidity cutoff can be accurately represented by a single value, namely the vertical cutoff rigidity. This ignores the presence of fluctuations in the planetary magnetic field, as well as the change in the cutoff as one propagates through a larger atmospheric overburden. Additionally, the spatial distribution of protons from the event is assumed to be isotropic. This is a reasonable assumption since it has been shown by Lovell et al. (1999) that the distribution was nearly isotropic by the time of maximum intensity, which is the time that is being analyzed here.

After obtaining the range of spectral parameters from the Milagrito data, we compared this to the spectrum obtained by the world wide network of neutron monitors. Neutron monitor data for this proton event, near the time of maximum intensity, indicate a rigidity power-law spectral index between approximately 5.2 and 6 in the 1-4 GV rigidity range (Duldig et al. 1999, Lovell et al. 1999). If the Milagrito derived range of spectral parameters for protons above 4 GV includes the neutron monitor spectrum at this rigidity, then a unique solution for the spectrum above 4 GV can be obtained. Doing this, we found that the index $\alpha = 9.0 \pm 2.3$ best fits the data. (The error is dominated by the error in the calculated effective area. Statistical errors from background fluctuations and errors arising from the fitting technique are also included. The error bars for the spectral parameters are obtained by doing the above integral with the input parameters modified by their 1σ error bars.) The analysis leading to this spectral index assumes a single power law above 4 GV. We also performed the analysis with the allowance of a hard upper cutoff at an energy which is varied as a free parameter. In order for the Milagrito scaler data and the neutron monitor data to be consistent, the hard cutoff must occur at 4.7 ± 0.5 GV, if we assume that the $P^{-5.2}$ spectrum of Lovell et al. (1999) extends into the energy range of Milagrito. In either case, these results indicate a cutoff or a rollover in the spectrum in the transition region between the neutron monitors and Milagrito. This is most likely of the form of a progressive spectral softening throughout the energy region above ~1 GeV.

Event Timing

Prior to the detection of energetic particles at Earth, X-rays and gamma rays were detected by space-based instruments, and the CME-associated solar flare was categorized as X9. Yoshimori reported the detection of gamma rays up to 100 MeV, with an onset time of 11:52 UT for the 10-20 MeV emission (Yoshimori et al. 2000). See figure 8. Several lines were present in the count spectrum derived from Yohkoh data, including the neutron capture line and C and O deexcitation lines. It is clear that proton acceleration was occurring at the flare site for a short period of time following 11:52 UT. The gamma ray event, as measured with Yohkoh, was over within five minutes of onset.

The time profile measured by Milagrito is consistent with that of Climax, when allowances are made for the long-term, background meteorological fluctuations (Figures

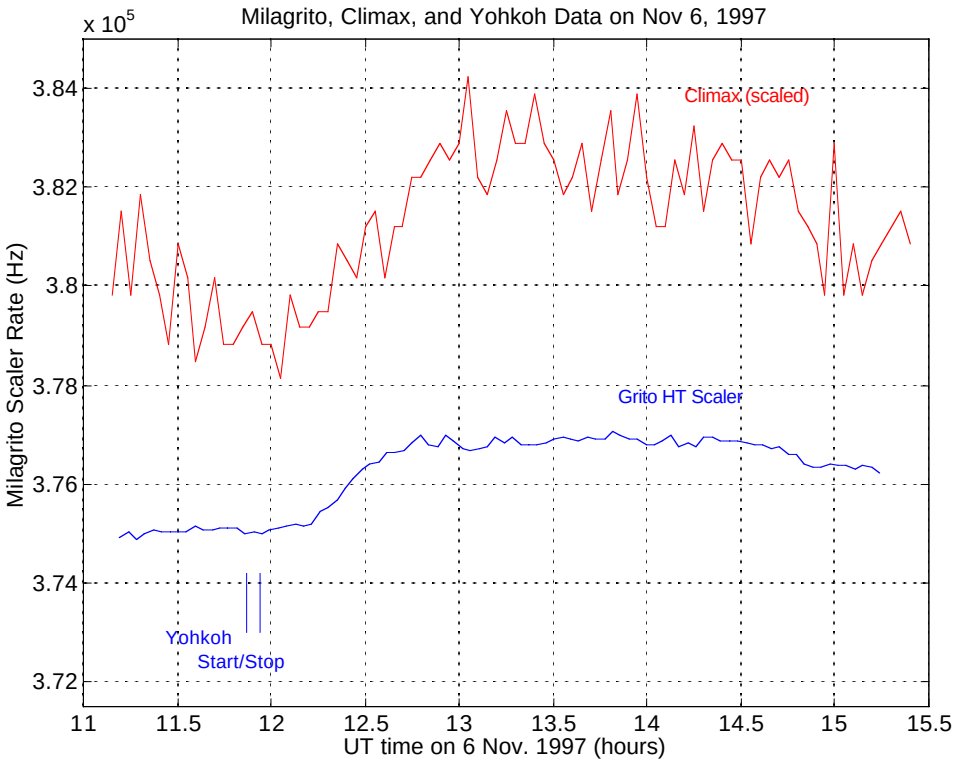

Fig. 8 – Onset of the Milagrito high threshold scaler rate increase and the Climax rate increase, with lines marking the beginning and end of the Yohkoh γ-ray line observations for comparison.

4 and 5). The onset of the Milagrito scaler rate enhancement, which was at 12:07 UT +/- 6 min, was simultaneous within error with the Climax neutron monitor onset time, which was at approximately 12:06 UT. The times of maximum intensity and the duration are also similar. The rate increase in Milagrito's scalers reached its maximum value at 12:44 UT ± 6 min. The GOES satellite observed an enhanced rate of protons from this event at about the same time. The >100 MeV proton emission detected by the GOES satellite lasted more than two days. GOES also detected protons from an event that occurred on 4 November. While the >100 MeV protons had returned to their pre-disturbance flux by

the time of the 6 Nov. event, the >10 MeV flux of protons was still elevated over background by ~10x, relative to its value prior to the 4 Nov. event.

Discussion and Conclusions

When the short duration (~5 min) of the gamma ray line emission and the long duration (~hours to ~days, depending on energy) of the high energy proton acceleration are considered, it appears as though much of the proton acceleration is not from the flare site. Protons do appear to be accelerated at the flare site during the impulsive phase, but the GeV protons, which come later, probably originate in the low corona. If a CME driven shock was responsible for the GeV protons, then the height of the CME at the time at which protons reached these high energies can be estimated by looking at the difference in time between the gamma ray onset and the GLE onset, while accounting for the proton path length along the Parker spiral of the interplanetary magnetic field. This leads to an estimate of ~10 minutes for the acceleration time of the >4 GV protons. After this amount of time, assuming a CME leading edge speed of ~2000 km/s, the leading edge of the CME was at ~2 solar radii. This spatial scale is reasonable, and it is consistent with prior results on GeV ion acceleration heights found for the 24 May 1990 CME event studied by Lockwood et al. (1999) and the September 1989 event studied by Kahler (1992). In these studies, which made use of similar timing arguments, particle injection heights were calculated to be ~2 solar radii and ~2.5-4 solar radii, respectively. An acceleration time of ~10 minutes for ~1-10 GeV protons is consistent with the collisionless shock model of Lee & Ryan (1986), when injection energies of ~10 MeV are present. While this is a simple blast wave model, similar driven shock models could be applied (e.g. Lee 1997). Based on GOES data, there was an abundance of >10 MeV protons “leftover” from the 4 November solar event. These ambient energetic protons could have provided the >10 MeV injection energies needed by the propagating CME-driven shock. While this does present a consistent interpretation, it is not definitive.

Between 10 and 60 MeV, the instruments on board the ACE satellite observed a proton spectrum of the form $E^{-2.1}$ (Cohen et al. 1999), while at higher energies, ground-based instruments observed much softer spectra. The Milagrito data, combined with neutron monitor data, leads to a proton spectrum with a rigidity power law spectral index of 9.0 ± 2.3, if a single power law is assumed above ~4 GV. A continuation of the $P^{-5.2}$ spectrum from Lovell et al. (1999) with a hard cutoff is also possible. These spectra are, by construction, continuous with the spectrum derived from the world wide neutron monitor network at 4 GV. In any case, the spectra derived from Milagrito and neutron monitor data indicate a gradual rollover or a cutoff somewhere in Milagrito’s sensitivity range above ~4 GV.

The Milagro instrument, for which Milagrito was a prototype, is currently taking data. With its increased number of PMTs, multiple layer design, and increased effective area, Milagro may provide exciting results in the future. Proposed enhancements, which would allow Milagro to reconstruct hadronic events down to primary energies of ~5 GeV,

may increase Milagro's capabilities to study solar energetic particles in the future (Ryan et al. 2000).

Acknowledgements

This work was supported in part by the National Science Foundation, the US Department of Energy Office of High Energy Physics, the US Department of Energy Office of Nuclear Physics, Los Alamos National Laboratory, the University of California, the Institute of Geophysics and Planetary Physics, the Research Corporation, the California Space Institute, and the University of New Hampshire Space Science Center.

References

Atkins, R., et al. 2000, *Nuclear Instruments & Methods in Physics Research A*, **449**, 478.
CERN Application Software Group 1994, CERN W, 5013, Version 3.21.
Chiba, N., et al. 1992, *Astroparticle Physics*, **1**, 27.
Cohen, C.M.S., et al. 1999, *Geophys. Res. Lett.*, **26**, 149.
Duldig, M.L. and Humble, J.E. 1999, in *Proc. XXV! Int. Cosmic Ray Conf*, **6**, 403.
Falcone, A.D., et al. 1999, *Astroparticle Physics*, **11**, 283.
Fowler, G.N., Wolfendale, A.W., and Flugge, S., eds. 1961, *Cosmic Rays I*.
Gosling, J.T. 1993, *Journ. of Geophys. Research*, **98** (A11), 18937.
Hayakawa, S. 1969, *Cosmic Ray Physics* (New York: John Wiley and Sons).
Heck, D. 1999, *private communication*
Heck, D., et al. 1998, *Corsika: A Monte Carlo Code to Simulate Extensive Air Showers*, Forschungszentrum Karlsruhe Report FZKA 6019.
Kahler, S.W. 1994, *Astrophys. J.*, **428**, 837.
Kahler, S.W. 1992, *Annu. Rev. Astron & Astrophys.*, **30**, 113.
Lee, M.A. 1997, in *American Geophys. Union Monograph 99: Coronal Mass Ejections*, eds. Crooker, N., Joselyn, J., & Feynman, J., 227.
Lee, M.A., and Ryan, J.M. 1986, *Astrophys. J.*, **303**, 829.
Lockwood, J.A., Debrunner, H., Ryan, J.M. 1999, *Astroparticle Physics*, **12**, 97.
Lovell, J.L., et al. 1999, *Adv. Space Res.*
Lovell, J.L., Duldig, M.L., Humble, J.E. 1998, *Journ. of Geophys. Research*, **103**, 23733.
Mason, G.M., et al. 1999, *Geophys. Res. Lett.*, **26**, 141.
McCullough, J.F., et al. 1999, in *Proc. XXVI Int. Cosmic Ray Conf.*, **2**, 369.
Meyer, P., Parker, E.N., Simpson, J.A. 1956, *Physical Review*, **104**, 768.
Mobius, E, et al. 1999, *Geophys. Res. Lett.*, **26**, 145.
Parker, E.N. 1957, *Physical Review*, **107**, 830.
Reames, D.V. 1999, *Space Science Reviews*, **90**, 413.
Ryan, J.M. et al. 2000, in *AIP Conf. Proc. 528: Acceleration and Transport of Energetic Particles Observed in the Heliosphere*, eds. Mewaldt, R.A., et al., 197.
Ryan, J.M. et al. 1999, in *Proc. of the XXVI International Cosmic Ray Conf.*, **6**, 378.
Yoshimori, M., et al. 2000, in *AIP Conf. Proc. 528: Acceleration and Transport of Energetic Particles Observed in the Heliosphere*, eds. Mewaldt, R.A., et al., 189.